Space-time Grid Connections for Finite Integration Method

Kota Arai, Takeshi Mifune, *Member, IEEE,* Tetsuji Matsuo, *Member, IEEE*

Graduate School of Engineering, Kyoto University, Kyoto 615-8510, Japan, araikota@fem.kuee.kyoto-u.ac.jp

The perfectly matched layer (PML) absorbing boundary is implemented for the space-time finite integration (FI) method. The subgrid connection in 3D and 4D space-time is discussed. The computational accuracy of several types of 3D and 4D space-time subgrid methods are evaluated using the PML.

***Index Terms*— Boundary condition, electromagnetic wave absorption, finite integration method, time-domain analysis.**

I. Introduction

The electromagnetic field analysis of fine structure of sub-wavelength scale is required for advanced electronic and optical devices [1]. The analysis of these devices using the conventional FDTD method [2] suffers large computational cost because the spatial grid should be refined uniformly unless a sophisticated subgrid method [2] is used. The space-time finite integration (FI) method [3]-[4] achieves efficient electromagnetic field computation using an adaptive time-step. Ref. [5] developed 3D and 4D space-time subgrid method for the adaptive grid construction and compared with the subgrid scheme [6] derived from the spatial FI method [7]. However, the computational accuracy of space-time subgrid scheme has not yet been fully examined because only the periodic spatial boundary condition was implemented.

This paper develops the connection scheme to the perfectly matched layer (PML) [8] for the space-time FI method and discusses the 3D and 4D connections to space-time subgrids.

II. Space-time finite integration method

The coordinate system is denoted by $(w, x, y, z) = (x^0, x^1, x^2, x^3)$ where $w = ct$, $c = 1/\sqrt{\varepsilon_0\mu_0}$ and ε_0 and μ_0 are respectively the permittivity and permeability of vacuum. The integral forms of Maxwell equations [4] without source terms are

$$\oint_{\partial\Omega_p} F = 0, \oint_{\partial\Omega_d} G = 0, \tag{1}$$

$$F = -\sum_{i=1}^{3} E_i \mathrm{d}x^0 \mathrm{d}x^i + \sum_{j=1}^{3} cB_j \mathrm{d}x^k \mathrm{d}x^l\,, \tag{2}$$

$$\mathrm{G} = \sum_{i=1}^{3} H_i \mathrm{d}x^0 \mathrm{d}x^i + \sum_{j=1}^{3} cD_j \mathrm{d}x^k \mathrm{d}x^l\,, \tag{3}$$

where (j, k, l) is a cyclic permutation of $(1, 2, 3)$, and Ω_p and Ω_d are hypersurfaces in space-time ; $\partial\Omega_p$ and $\partial\Omega_d$ are respectively constituted by the faces of primal and dual grids. The electromagnetic variables in the FI method are defined as

$$f = \int_{S_p} F\,, g = \int_{S_d} G, \tag{4}$$

where S_p and S_d are the faces of the primal and dual grids that constitute $\partial\Omega_p$ and $\partial\Omega_d$. To express the constitutive equation simply, the Hodge dual grid [4] is introduced as

$$\frac{\int_{Sd} c_r dx^0 dx^j}{\int_{Sp} dx^k dx^l} = -\frac{\int_{Sd} dx^k dx^l}{\int_{Sp} c_r dx^0 dx^j} = \kappa\,, \tag{5}$$

where $c_r = 1/\sqrt{\varepsilon_r\mu_r}$; κ is a constant determined for each pair of S_p and S_d ; and ε_r and μ_r are respectively the relative permittivity and permeability. From (4) and (5), it follows that $f = Zg/\kappa$, where $Z = \sqrt{\mu_r\mu_0/(\varepsilon_r\varepsilon_0)}$ is the impedance.

III. PML absorbing boundary condition

In the 3D space, all the components of electric flux density and magnetic flux density are divided into two subcomponents respectively such as

$$D_x = D_{xy} + D_{xz}\ . \tag{6}$$

Using these subcomponents, the space-time FI method updates the electric flux density in the PML as

$$d_{xy,i+\frac{1}{2},j-\frac{1}{2},k-\frac{1}{2}}^{\,n+\frac{1}{2}} = \frac{1-\frac{\Delta w}{2}\sigma_y\sqrt{\frac{\mu_0}{\varepsilon_0}}}{1+\frac{\Delta w}{2}\sigma_y\sqrt{\frac{\mu_0}{\varepsilon_0}}} d_{xy,i+\frac{1}{2},j-\frac{1}{2},k-\frac{1}{2}}^{\,n-\frac{1}{2}} + \frac{1}{1+\frac{\Delta w}{2}\sigma_y\sqrt{\frac{\mu_0}{\varepsilon_0}}}\left({h_{z,i,j,k}}^{n} - {h_{z,i,j-1,k}}^{n}\right),$$

$$d_{xz,i+\frac{1}{2},j-\frac{1}{2},k-\frac{1}{2}}^{\,n+\frac{1}{2}} = \frac{1-\frac{\Delta w}{2}\sigma_z\sqrt{\frac{\mu_0}{\varepsilon_0}}}{1+\frac{\Delta w}{2}\sigma_z\sqrt{\frac{\mu_0}{\varepsilon_0}}} d_{xz,i+\frac{1}{2},j-\frac{1}{2},k-\frac{1}{2}}^{\,n-\frac{1}{2}} - \frac{1}{1+\frac{\Delta w}{2}\sigma_z\sqrt{\frac{\mu_0}{\varepsilon_0}}}\left({h_{y,i,j,k}}^{n} - {h_{y,i,j,k-1}}^{n}\right), \tag{7}$$

where σ_y and σ_z are the electric conductivities in y-direction and z-direction respectively, Δw is the time-step, the subscripts are spatial indexes for x , y and z directions, and the superscript is the temporal index. The time-marching scheme for the other variables is given similarly.

IV. Space-Time Subgrid Connection

Ref. [5] proposed straight-type and staircase-type subgrids in the 3D and 4D space-time. However, the subgrid connection in 4D space-time was not discussed in detail.

A. 3D space-time subgrid

The 3D straight-type and staircase-type space-time subgrids are examined with the PML boundary condition. Fig. 1 illustrates the computational domain, where Δx and Δw are set to 1 and 0.5 by normalization and Δl is a free parameter. The normalized initial conditions are $E_x = E_y = 0$ and $B_z = \exp[-(x^2 + y^2)/25]$. Fig. 2 depicts the distributions of discrepancy ΔB_z between B_z obtained employing FDTD

method and that obtained using the 3D staircase-type space-time subgrid at ct = 100. Unphysical wave reflection caused by the subgrid connection is reduced by the optimization of Δl.

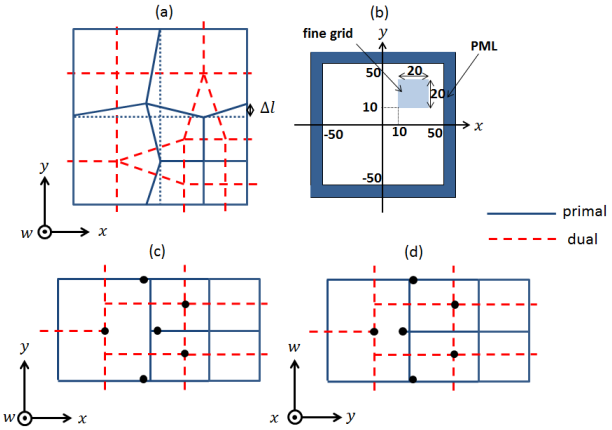

Fig. 1. 3D Space-time subgrid: (a) the straight type subgrid with a free parameter Δl, (b) computational domain, and (c) spatial and (d) space-time subgrid connection of staircase type.

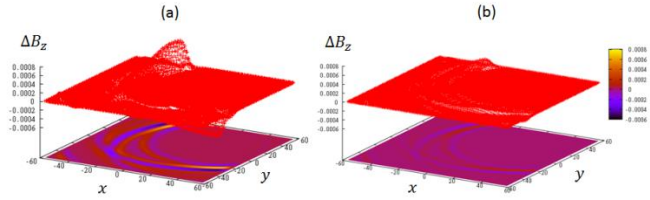

Fig. 2. Discrepancy of B_z compared with FDTD method: (a)Δl = 0.01, and (b) Δl = 0.1.

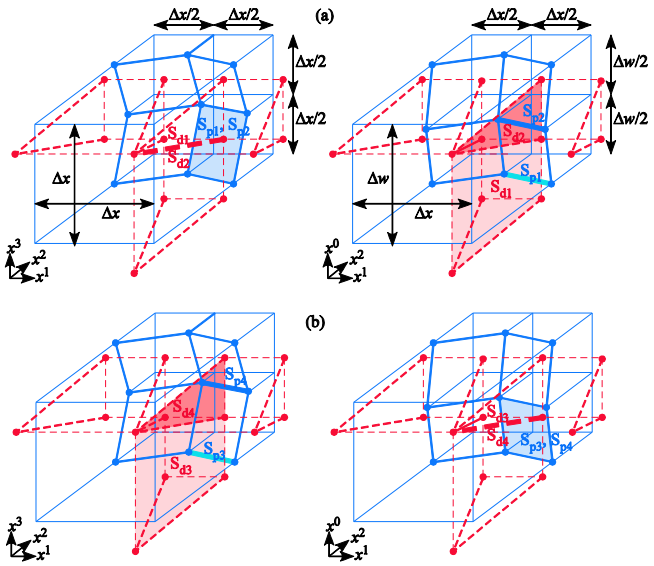

Fig. 3. 4D Straight type subgrid connection: (a) faces S_{p1}, S_{p2}, S_{d1}, S_{d2}, and (b) faces S_{p3}, S_{p4}, S_{d3}, S_{d4}.

B. 4D Strait type subgrid

Fig. 3 illustrates the straight-type subgrid connection. The faces S_{p1}, S_{p2} and their dual faces S_{d1}, S_{d2} are given as

$$S_{p1} = S_{p2} = \Delta x(dx_2/2 - dx_1/6) \wedge \Delta x(dx_3/2 + dx_1/6) \quad (8)$$

$$S_{d1} = 3\Delta w dx_0/4 \wedge \Delta x(3dx_1/4 + dx_2/4 - dx_3/4),$$

$$S_{d2} = \Delta w dx_0/4 \wedge \Delta x(3dx_1/4 + dx_2/4 - dx_3/4) \quad (9)$$

The variables $f_i = \int_{Spi} F$ (i = 1, 2) mean magnetic fluxes and $g_i = \int_{Sdi} G$ (i = 1, 2) mean magnetomotive forces such as:

$$f_1 = (\Delta x)^2(3cB_1 + cB_2 - cB_3)/12 \quad (10)$$

$$g_1 = 3\Delta x\Delta w(3H_1 + H_2 - H_3)/16. \quad (11)$$

The faces S_{p3}, S_{p4} and their dual faces S_{d3}, S_{d4} are given as

$$S_{p3} = [\Delta w dx_0/2 - (\Delta w)^2 dx_1/6\Delta x] \wedge \Delta x(dx_2/2 - dx_1/6),$$

$$S_{p4} = [\Delta w dx_0/2 - (\Delta w)^2 dx_1/6\Delta x] \wedge \Delta x(dx_2/2 - dx_1/6) \quad (12)$$

$$S_{d3} = [\Delta x(3dx_1/4 + dx_2/4) - \Delta w dx_0/4] \wedge 3\Delta x dx_3/4,$$

$$S_{d4} = [\Delta x(3dx_1/4 + dx_2/4) - \Delta w dx_0/4] \wedge \Delta x dx_3/4. \quad (13)$$

The dominant component of f_3 and f_4 is the electromotive force but f_3 and f_4 also contain magnetic flux such as:

$$f_3 = \Delta w[\Delta x(3E_2 - E_1) - \Delta w cB_3]/12. \quad (14)$$

The dominant component of g_3 and g_4 is the electric flux but g_3 and g_4 also contain magnetomotive force such as:

$$g_3 = 3\Delta x[\Delta x(-3cD_2 + cD_1) - \Delta w H_3]/16. \quad (15)$$

C. 4D Staircase type subgrid

Fig. 4 illustrates the staircase-type subgrid connection. The faces S_{pi} and their dual faces S_{di} (i = 1, …, 4) are redefined in the staircase type subgrid as

$$S_{p1} = (\Delta x)^2(dx_2dx_3/4 + dx_3dx_1/8 - dx_1dx_2/8),$$

$$S_{p2} = (\Delta x)^2(dx_2dx_3/4 + dzdx_0/24 - dx_1dx_2/24) \quad (16)$$

$$S_{d1} = \Delta x\Delta w(3dx_0dx_1/8 + 3dx_0dx_2/16 - 3dx_0dx_3/16),$$

$$S_{d2} = \Delta x\Delta w(3dx_0dx_1/8 + dx_0dx_2/16 - dx_0dx_3/16) \quad (17)$$

$$S_{p3} = \Delta x\Delta w(dx_0dx_2/4 - dx_0dx_1/8) - (\Delta w)^2 dx_1dx_2/8,$$

$$S_{p4} = \Delta x\Delta w(dx_0dx_2/4 - dx_0dx_1/24) - (\Delta w)^2 dx_1dx_2/24 \quad (18)$$

$$S_{d3} = (\Delta x)^2(-3dx_3dx_1/8 + 3dx_2dx_3/16) - 3\Delta x\Delta w dx_0dx_3/16,$$

$$S_{d4} = (\Delta x)^2(-3dx_3dx_1/8 + dx_2dx_3/16) - \Delta x\Delta w dx_0dx_3/16. \quad (19)$$

The computational accuracy given by the two types of subgrid connections will be compared in the full paper.

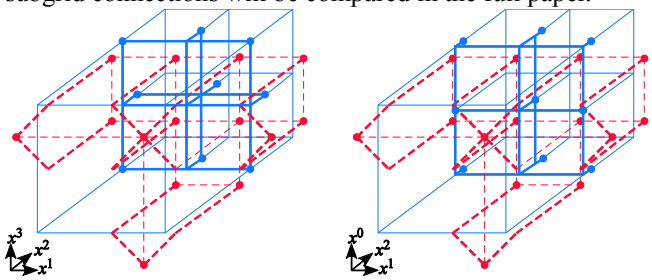

Fig. 4. 4D Staircase type subgrid connection.

V. REFERENCES

[1] Y. Hao and R. Mittra, "FDTD modeling of metamaterials: Theory and applications," *Artech House*, 2009.

[2] A. Taflove and S. C. Hagness, "Computational electrodynamics: The finite difference time-domain method," *Artech House*, 2005.

[3] T. Matsuo, "Electromagnetic field computation using space-time grid and finite integration method," *IEEE Tran. Magn.*, vol. 46, pp. 3241-3244, 2010.

[4] T. Matsuo, "Space-time finite integration method for electromagnetic field computation," *IEEE Trans. Magn.*, vol. 47, pp. 1530-1533, 2011.

[5] T. Matsuo, T. Shimoi, J. Kawahara, and T. Mifune, "A simple subgrid scheme using space-time finite integration method," *IEEE Trans. Magn.*, vol. 51, 7201904, 2015.

[6] P. Thoma and T. Weiland, "A consistent subgridding scheme for the finite difference time domain method," *Int. J. Numer. Model.*, vol. 9, pp. 359–374, 1996.

[7] T. Weiland, "Time domain electromagnetic field computation with finite difference methods," *Int. J. Numer. Model.*, vol.9, pp.295-319, 1996.

[8] J.-P. Berenger, "A perfectly matched layer for the absorption of electro-magnetic waves," *Journal of Computational Physics*, vol. 114, pp. 185-200, 1994.